# A Potential Biomarker in Sports-Related Concussion: Brain Functional Connectivity Alteration of the Default-Mode Network Measured with Longitudinal Resting-State fMRI over 30 Days

David C. Zhu[1,6,8], Tracey Covassin[2,7], Sally Nogle[2,7], Scarlett Doyle[1,8], Doozie Russell[3], Randolph L. Pearson[4], Jeffrey Monroe[2], Christine M. Liszewski[5], J. Kevin DeMarco[1], David I. Kaufman[3]

[1]Department of Radiology
[2]Department of Intercollegiate Athletics
[3]Department of Neurology and Ophthalmology
[4]Department of Family Medicine
[5]Department of Psychiatry
[6]Department of Psychology
[7]Department of Kinesiology
[8]Cognitive Imaging Research Center
Michigan State University

Address correspondence to:
David C. Zhu, Ph.D.
Radiology Building
Michigan State University
846 Service Road
East Lansing, MI 48824
Phone: (517) 884-3345
Fax: (517) 432-2849
Email: zhuda@msu.edu

Running title:

Concussion Default-Mode Network Resting-State fMRI

Keywords:

Default-mode network, resting-state fMRI, diffusion-tensor imaging, sports-related concussion, mild traumatic brain injury

## Abstract

Current diagnosis and monitoring of sports-related concussion rely on clinical signs and symptoms, and balance, vestibular and neuropsychological examinations. Conventional brain imaging often does not reveal abnormalities. We sought to assess if the longitudinal change of functional and structural connectivity of the default-mode network (DMN) can serve as a potential biomarker. Eight concussed Division 1 collegiate football student-athletes in season (one participated twice) and 11 control subjects participated in this study. ImPACT (Immediate Post-Concussion Assessment and Cognitive Testing) was administered over the course of recovery. High-resolution 3D $T_1$-weighted, $T_2$*-weighted, diffusion-tensor and resting-state fMRI (rs-fMRI) images were collected from each subject within 24 hours, $7 \pm 1$ and $30 \pm 1$ days after concussion. Both network-based and whole-brain based functional correlation analyses on DMN were performed. ImPACT findings demonstrated significant cognitive impairment across multiple categories and a significant increase of symptom severity on Day 1 following a concussion, but fully recovered by $6 \pm 2.4$ days. While the structural connectivity within DMN and gross anatomy appeared unchanged, a significantly reduced functional connectivity within DMN from Day 1 to 7 was found in the concussed group in this small pilot study. This reduction was seen in eight of our nine concussion cases. Compared to the control group, there appears a general trend of increased DMN functional connectivity on Day 1, a significant drop on Day 7, and partial recovery on Day 30. The results from this pilot study suggest that the functional connectivity of DMN measured with longitudinal rs-fMRI can serve as a potential biomarker to monitor the dynamically changing brain function after sports-related concussion, even in patients who have clinically improved.

## Introduction

Sports-related mild traumatic brain injury (mTBI), commonly referred to as sports-related concussion, has emerged as a major public health issue. There are 1.6 to 3.8 million sports-related traumatic brain injuries each year [1], with mTBI accounting for 80% of all traumatic brain injuries [2]. Current diagnosis and monitoring of concussion rely on clinical signs and symptoms, and balance, vestibular and neuropsychological examinations, with no validated consensus tests available [3]. The timing of a safe return to play for a concussed athlete essentially is based on these subjective evaluations [4]. Furthermore, although most concussions improve clinically within a few days [5-6], understanding the recovery process and long-term effect is challenging [7]. Conventional brain imaging such as CT and MRI scanning does not reveal measurable variation or abnormality acutely in concussion. The recently developed resting-state fMRI (rs-fMRI) [8] and diffusion tensor imaging (DTI) [9-11] MRI techniques, coupled with more traditional anatomical MRI techniques, offers the potential to provide objective biomarkers to determine the level of injury, monitor the recovery process and aid in return-to-play decisions.

Neuroscience has revealed that the brain operates in an efficient manner through highly organized networks. When a concussion occurs, the efficient organization of these networks becomes dysfunctional. Loss of consciousness (LOC) is the most dramatic event associated with concussion. However, LOC is only associated with approximately 9% of all concussions [12]. Subtle cognitive disturbances, mood disorders, sleep abnormalities, headache and systemic symptoms like nausea are also associated with the clinical syndrome of concussion, which can make the disorder challenging to diagnose. Since brain networks operate in a cohesive manner between connections and nodes, their disruption, as suggested by the symptoms, leads to the dysfunction of a whole network and potentially its relationship to other brain networks. The lack of sensitivity in CT and traditional MR brain imaging in the diagnosis of most concussion cases

suggests that the alteration of anatomical structure is subtle or difficult to diagnose, although the brain alteration is reflected by clinical neurologic examination and neuropsychological testing.

Recently, rs-fMRI has emerged as an effective way to investigate the integration of brain networks. In this technique, fMRI data are acquired when an individual is asked to do nothing but stay awake while lying in the MRI scanner. The rs-fMRI technique emerged based on the observed phenomena that approximately 95% of the brain's metabolism occurs due to spontaneous neuronal activity [8, 13]. This technique has demonstrated its potential applicability through a few studies in concussion research [14-21]. The functional connectivity of the default-mode network (DMN) was found reduced after concussion in these prior studies.

When the disruption of a functional connection is detected, it is important to understand whether it is due to axonal damage, which leads to the disruption of structural connection. The development of DTI [9-11] continues to enhance our understanding of neuronal structural connectivity *in vivo*, and its potential damage in concussion [22-24]. Two functionally connected regions must be directly or indirectly connected in structure. Abnormal neuronal function can be caused by damaged structural connections between neurons or damage to the neurons themselves. Therefore, an integration of functional connectivity based on rs-fMRI and structural connectivity based on DTI provides better understanding of the neural networks than one single connectivity analysis [25].

In sports-related concussion, the brain regions involved in physical impact are often difficult to predict. Hence, a brain network that is suitable as a biomarker would need to be sensitive to physical impacts on different brain locations. One such network is likely the DMN of the brain [26]. The DMN was first found to be disrupted in Alzheimer's disease [27-30] but recently also found to be disrupted in concussed patients [14, 16-18]. The DMN is characterized by

"deactivation" on fMRI during cognitively demanding tasks in normal subjects. As reviewed by Buckner et al. [31], the DMN includes the posterior cingulate cortex (PCC), medial prefrontal cortex (MePFC), temporoparietal junction cortices (TPJC) (including some regions in inferior parietal lobule, lateral temporal cortex, angular gyrus and supramarginal gyrus) and regions of the medial temporal lobe (MTL) (including the hippocampal formation, entorhinal cortex and parahippocampal gyrus (PHG)). These regions appear to be active in synchrony when the brain is "at rest". Of note, the cingulum bundle interconnects multiple components of the DMN, including the MePFC, PCC, and MTL [32]. The MTL processes information from prior experiences in the form of memories. The MePFC facilitates the flexible use of this information during the construction of self-relevant mental simulations, and the outputs of these two regions converge on the PCC for information integration [31]. Consequently, the structural and/or functional damage of these brain regions can lead to cognitive impairment. These regions are distributed in multiple lobes of the brain and connect across the hemispheres. Neuronal damage due to physical impact, although not well defined, likely leads to some alteration of the DMN.

Previous studies focused on the investigation of the disruption of DMN brain connectivity after concussion by sampling brain imaging data on one time point [14-16] or with more than one time point but no data during the early acute phase (< 3 days) after concussion [17-18]. In this study, we investigated the longitudinal change of brain connectivity within 24 hours of concussion, then 7 and 30 days. We also integrated the functional and structural connectivity analyses. We tested the hypothesis that the functional connectivity of the DMN would dynamically change over the course of recovery after concussion, but its structural connectivity and anatomical structure would remain relatively stable. We wanted to test the secondary hypothesis that the functional connectivity to PCC, the hub region of the DMN, would dynamically change over the course of

the recovery and to explore the alteration of other regions within the DMN. We also wanted to test the feasibility of carrying out a longitudinal neuroimaging study in active Division 1 football student-athletes in season.

## Methods

*Subjects*

Eight male collegiate concussed football student-athletes in season (20 ± 1.3 years old, one repeated case) and 11 male control subjects (20.5 ± 1.8 years old) participated in this study. The repeated concussed case was not entered in group analyses, but was only used in the post-hoc evaluation to assess the fraction of cases that follow the trend of DMN alteration found in group analyses. All concussed athletes had symptoms immediately post injury. None of the concussions happened in an away game. None of the concussed subjects were in air travel before the Days 1 and 7 MRI scans, and 48 hours before the Day 30 MRI scan. The control subjects were college students at a comparable age range as the student-athletes, and met the American College of Sports Medicine (ACSM) guidelines for physical activity (Cardio-respiratory exercise—at least 150 minutes of exercise with moderate intensity or 75 minutes of exercise with vigorous intensity per week). Participants also met one of the following two recommendations: resistance exercise—two to four sets of 8-12 repetitions on major muscle group such as chest, shoulders, back, hips, legs, trunk, and arms two or three days per week using a variety of exercises and equipment, or neuromotor exercise—two or three days per week of exercises that involves motor skills (balance, agility, coordination and gait). All subjects self-reported that they were free of neurological issues besides concussion during the period of participation. All subjects signed consent forms approved by the Michigan State University Institutional Review Board.

*Neuropsychological Tests*

To assess neurocognitive function, the online version of the Immediate Post Concussion Assessment Cognitive Testing (ImPACT) neuropsychological test battery [33] was used for this study. The ImPACT test takes about 25 minutes. It includes a symptom scale and six neurocognitive test modules. The test scores are then used to calculate four composite scores including verbal memory, visual memory, motor processing speed, and reaction time. The detailed description of ImPACT as well as its test-retest reliability, validity, and specificity/sensitivity are reported elsewhere [33-36]. ImPACT was administered to concussed athletes prior to the start of their preseason which constituted their baseline test. ImPACT was then administered on Day 1, and every 2-3 days until the athlete returned to their baseline scores (around Day 7). Repeated measures ANOVAs on three time points (baseline, Day 1 and around Day 7) for each of the four composite scores and the total symptom score were conducted to evaluate neurocognitive performance after a concussion.

*Operational Definition of Concussion*

Concussion was operationally defined using the definition recommended by the 4th International Concussion in Sport Group as "a complex pathophysiological process affecting the brain, induced by biomechanical forces" [37]. A concussion was required to meet the following two criteria in this study: (1) presence of on-field signs (e.g., post-traumatic amnesia, loss of consciousness) and symptoms (e.g., dizziness, headache, nausea) as determined by a sports medicine physician (RP and DK) or a neurologist (DK), and (2) decrease from baseline in at least one of the four ImPACT composite scores by a clinically significant magnitude.

*MRI Acquisition*

The MRI experiment was conducted on a GE 3T Signa® HDx MR scanner (GE Healthcare, Waukesha, WI) with an 8-channel head coil. High-resolution 3D $T_1$-weighted, $T_2$*-weighted, DTI and rs-fMRI brain images were collected from each subject within the first 24 hours, on $7 \pm 1$ days and then $30 \pm 1$ days after concussion, except one subject who was scanned on Day 77 rather on Day 30 due to winter break and class commitment at the beginning of the semester. In our data analyses, this single Day 77 data point was not included. Specifically, when only comparing Days 1 and 7, all subjects were included. In the comparisons of other days, this subject was not included. MRI data from the control subjects were collected at three time points with the same time intervals as the concussed subjects. During each scan session, first and higher-order shimming procedures were carried out to improve magnetic field homogeneity. To study resting-state brain function, two 7-min echo-planar imaging datasets, starting from the most inferior regions of the brain, were acquired with the following parameters: 38 contiguous 3-mm axial slices in an interleaved order, time of echo (TE) = 27.7 ms, time of repetition (TR) = 2500 ms, flip angle = 80 °, field of view (FOV) = 22 cm, matrix size = $64 \times 64$, ramp sampling, and with the first four data points discarded. For each 7-min rs-fMRI dataset, each volume of slices was acquired 164 times while a subject was asked to relax, stay awake and keep his eyes closed. After the functional data acquisition, DTI images were acquired with a dual spin-echo echo-planar imaging (EPI) sequence for 12 minutes and 6 seconds with the following parameters: 48 contiguous 2.4-mm axial slices in an interleaved order, FOV = 22 cm $\times$ 22 cm, matrix size = $128 \times 128$, number of excitations (NEX) = 2, TE = 77.5 ms, TR = 13.7 s, 25 diffusion-weighted volumes (one per gradient direction) with $b$ = 1000 s/mm$^2$, one volume with $b$ = 0 and parallel imaging acceleration factor = 2. Finally, 180 $T_1$-weighted 1-mm$^3$ isotropic volumetric inversion recovery fast spoiled gradient-recalled images (10 minute scan time), with

cerebrospinal fluid (CSF) suppressed, were obtained to cover the whole brain with the following parameters: TE = 3.8 ms, TR of acquisition = 8.6 ms, time of inversion (TI) = 831 ms, TR of inversion = 2332 ms, flip angle = 8 °, FOV = 25.6 cm × 25.6 cm, matrix size = 256 × 256, slice thickness = 1 mm, and receiver bandwidth = ± 20.8 kHz. $T_2$*-weighted gradient echo images were collected at the same slice locations of the fMRI dataset with the following parameters: 38 contiguous 3-mm axial slices, TE = 15 ms, TR = 850 ms, flip angle = 20 °, FOV = 22 cm × 22 cm, matrix size = 256 × 224, and receiver bandwidth = ± 20.8 kHz. All acquired structural images were visually inspected by an MRI physicist (DCZ) to guarantee high image quality in terms of signal-to-noise ratio (SNR) and image artifacts. The temporal SNR of the fMRI data was calculated and inspected to have good full-brain coverage (> 40 in general and > 100 in deep brain tissue). The rigid motion should be less than 4 mm based on the motion derivatives in the three translational and three rotational directions estimated in the resting-state fMRI pre-processing procedure as described in the next section. Small amount of motion was expected to be corrected through the motion correction procedure. No subject was rejected based on image quality. The alignment of the rs-fMRI, DTI and $T_1$-weighted high-resolution images was visually inspected. The "flirt" alignment software in FSL[38] was applied with six-degree of freedom to the $T_1$-weighted images to improve its alignment with rs-fMRI and DTI if necessary.

*Resting-State fMRI Individual-Subject Data Pre-Processing*

Resting-state fMRI correlation analysis was conducted using AFNI software [39] in the native space. For each subject, the acquisition timing difference was first corrected for different slice locations. With the last functional volume of the second run as the reference, rigid-body motion correction was done in three translational and three rotational directions. The motion derivatives in these six directions at each time point were estimated and then modeled as regressors in data

analysis. For each subject, spatial blurring with a full width half maximum (FWHM) of 4 mm was used to reduce random noise and inter-subject anatomical variation during group analysis. At each voxel, motion derivatives related signal changes, baseline, linear and quadratic system-induced signal trends were removed from the time courses using the "3dDeconvolve" routine in AFNI [40]. Brain global, CSF and white matter (WM) mean signals were modeled as nuisance variables and removed from the time courses as well. In order to create the time course from pure CSF regions, the lateral and 3rd ventricles on the high-resolution $T_1$-weighted volumetric images were segmented using FreeSurfer software followed by 1 $mm^3$ erosion [41]. For the same reason, the WM was segmented from the $T_1$-weighted volumetric images using the "FAST" routine in the FSL software [38] followed by 4 mm $\times$ 4 mm $\times$ 4 mm cubical erosion. The cleaned time courses were then band-pass filtered in the range of 0.009 Hz – 0.08 Hz [42]. The filtered time courses from two runs were concatenated. These concatenated time courses were entered the correlation-based connectivity analyses following.

*Network-Based Functional Connectivity Analyses on DMN*

To achieve unbiased functional network analyses, the nodes of a network need to be defined first in an unbiased manner. The cortical nodes of the DMN were extracted from the functional networks produced by Yeo et al. [43] based on rs-fMRI datasets from 1,000 healthy young adults. Besides the large sample size, the age range of this population matches well with the student-athletes we are studying. The group averaged cortical surface map of DMN in FreeSurfer [41] was provided by Yeo et al. [43]. We segmented this surface map to the following eight nodes according to the clustering characteristics and anatomical region: right and left posterior cingulate cortices (PCC), right and left anterior cingulate cortices (ACC)/medial frontal cortices (MeFC), right and left superior frontal gyri (SFG), and right and left inferior parietal

lobules (IPL)/angular gyri (AG). The small region at the right inferior lateral temporal cortex in Yeo's map is not a well defined DMN region [31], and thus was not included as a node in this study. The MTL is considered part of the DMN [31], but it is a sub-cortical region and thus was not defined in Yeo's work [43]. However, the hippocampus is the core of the MTL node and thus applied to represent MTL. All above 10 nodes (shown in Fig. 1), including the right and left hippocampi, were warped to the native space in each subject in FreeSurfer. At each node, the filtered time courses across all voxels within the node described earlier were then averaged to generate the mean time course. The Pearson correlation coefficient between each pair of mean time courses at two nodes were calculated with the "3dfim+" routine in AFNI [39]. To estimate two higher levels of connectivity, the mean correlation coefficient between one node and other nodes of DMN and the mean correlation coefficient of all connection pairs of DMN (overall connectivity) were also calculated. In addition, for the control group, the mean correlation coefficient across the three time points for each pair of nodes was also calculated. Then the two higher levels of connectivity were calculated as just described.

To prepare for group analyses, the correlation coefficients were converted to Z values through Fisher's Z-transformation to improve the normality of the distribution. For the preliminary analyses, we ran a "2 groups $\times$3 time points" ANOVA on the connectivity of the overall DMN and to each node to assess whether there were significant Group $\times$Time interactions. To understand the details of longitudinal change in each group, we first performed repeated measure ANOVA on the connectivity of the overall DMN and to each node, followed with post-hoc 2-tail paired *t* tests between each pair of measurement time points on each level of connectivity described earlier. To understand the difference between each time point in the concussed subjects and the control subjects (mean across three time points to reduce the effect of

fluctuation), 2-tail 2-sample *t* tests were performed. The DMN network is approximately 9.6% of the total size of the 17 functional networks produced by Yeo et al. [43], with the hippocampi included. Based on this percent size, to achieve a significant corrected $p \leq 0.05$ after Bonferroni correction, the statistical significance level needs to be set at $p \leq 0.0052$. After the overall DMN connectivity was found significantly changed, to locate a node that contributes to this change, the significance level was set at $p \leq 0.005$ to correct for multiple comparison. Since there are 10 nodes in the DMN, to achieve a significant corrected $p \leq 0.05$ after Bonferroni correction, significance level needs to be set at $p \leq 0.005$. Since neuropsychological and clinical tests have demonstrated the change of mental status after concussion, it can be too conservative to carry further Bonferroni correction in time.

*Seed Generation for Integrated Whole-Brain Connectivity Visualization and Analyses*

PCC is the hub of the DMN. The right and left isthmuses of the cingulate cortex (ICCs) are anatomically well defined regions within PCC based on FreeSurfer [41] segmentation, and were selected as seeds for whole-brain connectivity analyses on DMN in this work, as successfully demonstrated in Alzheimer's disease research [25]. To obtain the corresponding structural connectivity, WM regions immediately subjacent to the ICCs were used as seed regions for DTI fiber tracking. These WM regions were defined using FreeSurfer [41] to include WM tissue within 5 mm of the gray/white matter boundary. This approach allows for integrated understanding of the functional and structural connectivity from a common anatomical region.

*Functional Connectivity between Isthmuses of Cingulate Cortex and Rest of the Brain*

The "3dfim+" routine in AFNI [39] was used to correlate the time course in every voxel of the brain against the space-averaged time course from a seed region. To prepare for group analysis, the correlation coefficients were converted to Z values through Fisher's Z-

transformation to improve the normality of the distribution. After warping the Z values to the Talairach standard space, an ANOVA was performed for each group for within-group analyses with a mixed-effect two-factor model. The date of measurement was the first factor and was modeled as a fixed effect. Subject was the second factor and was modeled as a random effect.

Monte Carlo simulation was performed according to the matrix and voxel size of the imaging volume, brain masks generated by voxel intensity thresholding, and spatial smoothness of image data inherited and applied. The spatial smoothness of image data was estimated based on "3dFWHMx" in AFNI [39]. The cluster analysis was used to estimate the overall statistical significance with respect to the whole brain [44]. The between-group *t*-test results for functional connectivity with ICC were corrected for multiple comparisons based on the following criteria: A voxel was considered significant only if it was within an 1170 $mm^3$ cluster in which the voxels were connected and all had a voxel-based $p \leq 0.005$. Based on the application of these criteria to the whole brain, the voxel-based $p \leq 0.005$ was corrected to be an equivalent whole-brain corrected $p \leq 0.047$.

*Structural Connectivity from Isthmuses of Cingulate Cortex to Rest of the Brain*

Probabilistic fiber tracking was performed using routines from the FSL Diffusion Toolbox (FDT v2.0) [10, 38, 45]. After eddy-current distortion and motion correction, Bayesian Estimation of Diffusion Parameters Obtained using Sampling Techniques with crossing fibers modeled (n = 2) (BEDPOSTX) [10] was performed at each voxel. Then, probabilistic tractography with the "PROBTRACKX" routine was applied to calculate whole-brain connectivity distributions from each ICC seed region. The connectivity distribution maps were then warped to the Talairach standard space. Before group analyses, spatial blurring with FWHM of 2 mm was used to reduce

random noise and inter-subject anatomical variation. ANOVA was performed on the concussed group with a mixed-effect two-factor model as in the functional connectivity analyses.

For DTI structural connectivity, the between-group *t*-test results were similarly corrected for multiple comparisons based on Monte Carlo simulation as for functional connectivity. In this Monte Carlo simulation, the effect of both the inherited smoothness and the 2-mm FWHM spatial blurring applied was estimated. The average inherited smoothness of the raw DTI images collected from all subjects was estimated based on the "3dFWHMx" software with the "2difMAD" option in AFNI [39]. This inherited smoothness of the DTI images is expected to propagate to the connectivity distribution maps which would be used for group analyses. Based on Monte Carlo simulation, a voxel was considered significant only if it was within a 213 $mm^3$ cluster in which the voxels were connected and all had a voxel-based $p \leq 0.005$. Based on the application of these criteria to the whole brain, a voxel-based $p \leq 0.005$ was corrected to an equivalent whole-brain corrected $p \leq 0.048$.

*Neuronal Fiber Integrity Evaluation with Track-Based Spatial Statistics (TBSS) on DTI Metrics*

The Track-Based Spatial Statistics (TBSS) procedure in FDT of FSL[38] was applied to diffusion metrics (FA (fractional anisotropy), MD (mean diffusivity), AD (axial diffusivity) and RD (radial diffusivity)) from DTI to assess white-matter integrity. Specifically, all FA images were aligned to the ICBM-DTI-81 white-matter atlas developed by Mori et al.[46]. The FA skeleton mask was created with a threshold of > 0.2 on the FA skeleton. This FA skeleton mask was divided to 48 anatomical regions based on the ICBM-DTI-81 white-matter atlas. Repeated measure ANOVAs on FA/MD/RD/AD were applied to the overall skeleton and the 48 sub-regions, followed with post-hoc 2-tail paired *t* tests between each pair of measurement time

points on the concussed subjects. Assuming that the white matter was affected by a concussion, no multiple comparison correction would be needed for the overall skeleton, and thus the significance level can be set at $p \leq 0.05$. Since there are 48 regions in the ICBM-DTI-81 white-matter atlas, to achieve a significant corrected $p \leq 0.05$ after Bonferroni correction, significance level needs to be set at $p \leq 0.001$ for each region.

*Clinical Evaluation on Anatomical Images after Concussion*

A neuroradiologist (JKD), along with an MRI physicist/neuroscientist (DCZ), reviewed the anatomical images (3D $T_1$-weighted and $T_2$*-weighted images) collected over the three time points to qualitatively assess the potential anatomical abnormalities on the concussed and normal subjects based on his clinical expertise.

## Results

*Neuropsychological Tests*

Concussed athletes in this study exhibited impairment on visual memory composite score (*Wilk's* $\lambda$=.24, $F_{(2,7)}$ = 11.33, $p$=.006), motor processing speed composite score (*Wilk's* $\lambda$=.27, $F_{(2,7)}$ = 9.50, $p$=.01) and reaction time composite score (*Wilk's* $\lambda$=.26, $F_{(2,7)}$ = 9.90, $p$=.009), and had greater total symptom score (*Wilk's* $\lambda$=.28, $F_{(2,7)}$ = 9.14, $p$=.011) on Day 1 post-concussion compared to baseline. There was no significant difference on verbal memory composite score (*Wilk's* $\lambda$=.48, $F_{(2,7)}$ = 3.72, $p$=.079) in the concussed athletes compared to baseline. On Day 6 ± 2.4 days, the scores of the concussed athletes either recovered to or became better than their baseline measurements (Table 1).

*Network-Based Functional Connectivity Analyses on DMN*

There were significant Time × Group interactions on the functional connectivity of the overall DMN ($p = 0.002$), left hippocampus ($p < 0.001$), right hippocampus ($p < 0.001$) and right PCC ($p = 0.001$). The left PCC was approaching significance ($p = 0.007$). The uncorrected *p* values are listed. The functional connectivity of the DMN overall was significantly higher on Day 1 compared to Day 7 in the concussed group (Table 2). There was also a trend of increased (although not significant) functional connectivity on Day 30 compared to Day 7 based on the mean connectivity (correlation coefficient) to each node of DMN, as well as the DMN overall in the concussed group (Fig. 2). The mean DMN connectivity reductions from Day 1 for the concussed group (n = 7) were 51.8% on Day 7 and 27.5% on Day 30. The connectivity to the right or left PCC from the rest of the DMN in the concussed group was significantly reduced (after Bonferroni adjustment) from Day 1 to Day 7. The trend of connectivity reduction is also noted in all other nodes. The notable large effect sizes (based on the standardized mean difference Hedges' g) on the overall DMN (1.695), left PCC (1.739), right PCC (1.819) as well as other nodes can be seen on the paired *t* tests comparing Day 1 and Day 7 (Table 2). These results nicely correspond with Fig. 3. In this figure, the concussed group's functional connectivity (mean correlation coefficient) between each pair of nodes within the DMN and the paired *t* test results on Z values of correlation coefficient are shown for the data collected on the three separate days. The concussed group had the largest number of pairs of nodes with apparent connectivity reduction ($p \leq 0.05$ before corrected) occurring between Day 1 and Day 7, with a reduced number between Day 1 and Day 30, and much smaller number between Day 7 and Day 30. In comparison, the DMN functional connectivity overall of the control group was not significantly different between the three days (Table 3). The fluctuations of mean correlation coefficients were less than 9%. The effect sizes were less than 0.4 on the overall DMN, and in

general less than 0.5 in all nodes for all three paired *t* tests on the three measurement days. The pairs of nodes with apparent differential connectivity ($p \leq 0.05$ before corrected) between Day 1 and Day 7 and between Day 1 and Day 30 are notably much less than the corresponding comparisons in the concussed group (Fig. 4).

Compared to the control group (Table 4), the concussed group was found to have a significantly reduced DMN functional connectivity on Day 7, specifically on the overall DMN and on left and right SFG, left and right hippocampi, and right IPL/AG, all with large effect sizes (Hedges' $g > 1.45$). Significant differences were not found on Day 1 or Day 30 after concussion. Compared to the control group, based on the mean correlation coefficients (Tables 2 and 4), the DMN overall connectivity of the concussed group was higher by 14.5% on Day 1, but lower by 41.4% on Day 7, and then recovered but still lower by 15% on Day 30 (Fig. 2).

*Functional Connectivity between Isthmuses of Cingulate Cortex and Other DMN Regions Based on Whole-Brain Analyses*

The ANOVAs of the concussed group showed a significantly reduced functional connectivity between left ICC and other DMN regions from Day 1 to Day 7, notably around MeFC, SFG, AG/MTG and hippocampus/PHG (Table 5 and Fig. 5). The significant reduction of functional connectivity from Day 1 to Day 30 was also found at the left SFG. There was also a trend of improved DMN functional connectivity between left ICC and other DMN regions from Day 7 to 30 (Fig. 5). At the PCC region surrounding left ICC, there was a significant reduction of functional connectivity to left ICC from Day 1 to Day 7 (Table 5).

Similarly, the ANOVAs within the concussed group showed a significantly reduced functional connectivity between right ICC and other DMN regions from Day 1 to Day 7, notably around ACC, MeFC, SFG, AG/MTG/precuneus/superior occipital gyrus and hippocampus/PHG

(Table 6). However, ANOVAs of the concussed group between Day 1 and Day 30 and between Day 7 and Day 30 did not find significant clusters showing the change of connectivity between right ICC and the rest of DMN. ANOVAs of the control group did not find significant functional connectivity alteration of DMN between each pair of the three time points during one month.

*Structural Connectivity from Isthmus of Cingulate Cortex to Rest of DMN*

Significant structural connectivity difference between the right or left ICC and the rest of DMN (along the cingulum and around the WM adjacent to the DMN components) was not found comparing the three time points. The structural connectivity of DMN appeared relatively stable within the one-month period after concussion as demonstrated in the case study following.

*Longitudinal Alteration of Connectivity: a Representative Case*

This functional connectivity reduction between ICCs and the rest of DMN was seen in eight of our nine concussion cases. Fig. 6 shows a representative case with a longitudinal alteration of the functional connectivity to left ICC but the structural connectivity to left ICC appears unchanged. As noted, the size of the MeFC/ACC cluster (in green) that is connected to left ICC ($R > 0.4$) is largest on Day 1. With the same $R$ threshold, the cluster size is much smaller on Day 7, and then there is some increase on the cluster size on Day 30. The neuronal fibers (in orange) stretched from the left ICC remain visually unchanged, and remain strongly connected from ICC to MeFC/ACC. The change of structural connectivity from ICC along the cingulum appears very stable or subtle if there are changes, compared with the large scale on the modification of functional connectivity.

*Neuronal Fiber Integrity Evaluation with Track-Based Spatial Statistics (TBSS) on DTI Metrics*

For the concussed subjects, significant change of FA across time was found on the full white-matter skeleton, with effective sizes of 0.632 (1.7% change) between Days 7 and 30 and 0.674 (2 % change) between Days 1 and 30. However, significant changes of FA across time were not found on the 48 sub-regions of the white-matter skeleton (Table 7). Results on the cingulum and corpus callosum were selected to present to compare with prior findings[22-23]. Just based on the mean FAs, the changes across time in the cingulum and corpus callosum were less than 2.2%. Significant changes across the three time points were not found on the overall skeleton mask and the 48 sub-regions on diffusion metrics MD, RD and AD. On the right and left cingulum, the post-hoc paired *t* tests between time points showed effect sizes less than 0.4 on MD, RD and AD.

Visual inspection of the anatomical MR images did not find significant changes over the three time points from clinical perspectives on all concussed cases. One concussed subject demonstrated two anatomical abnormalities with a 5-mm $T_2$* hyper-intense/$T_1$ hypo-intense lesion in the right periventricular white matter as well as a 2-mm $T_2$* hyper-intense/$T_1$ hypo-intense lesion in the left posterior deep white matter, but both abnormalities were stable over the three time points. No significant clinical abnormality was found in the other eight cases. In the control group, there was one subject with an 8-mm cavernoma (stable over three time points) seen as a focal region of $T_2$* hypo-intensity in the right frontal lobe without edema. This abnormality was not at the DMN regions and thus this subject was included in the analyses.

## Discussion

It was previously considered logistically challenging to perform MRI scans within the first 24 hours after concussion and collect the associated longitudinal data, especially on Division 1

collegiate football student-athletes in season. Thus rs-fMRI longitudinal studies starting in the early acute phase (< 3 days) post concussion are not available in the literature. Our observed longitudinal change of functional connectivity measured with rs-fMRI starting at the very early acute phase might well be a biomarker in sports-related concussion. To our knowledge, this is the first neuroimaging study to track the longitudinal modifications of both functional and structural connectivity of the DMN starting from the first 24 hours after concussion until Day 30.

Concussed athletes' neurocognitive performance was significantly worse compared to baseline on Day 1 but returned to baseline levels by Day 7. This suggests the importance of collecting neuroimaging data within the first 24 hours after concussion. The findings from the current study on rs-fMRI confirm this importance. Specifically, both our network-based and seed-based whole-brain analyses demonstrate that there was a significantly higher functional connectivity within DMN on Day 1 than Day 7 after concussion, and Day 30 also by the latter analysis and a trend to significance by the formal analysis. The changes are clearly noted based on the percent changes (51.8% decrease from Day 1 to Day 7 and 50% rise from Day 7 to Day 30) and large effect sizes (1.695 Hedges'g comparing Day 1 to Day 7). The reduction from Day 1 to Day 7 was seen in eight of our nine individual concussed cases. Within DMN, the functional connectivity to PCC was most affected based on the unbiased network-based analyses. This result confirms the choice of using ICCs (the core region of PCC) for the seed-based whole-brain functional and structural connectivity analyses. Equivalent analyses on the control group did not find significant longitudinal alteration of DMN functional connectivity (less than 9% change with an effect size of < 0.5 in Hedges' g), suggesting that this dynamic functional connectivity alteration is specific to concussion. Assuming that the functional connectivity of each subject returns to the baseline level on Day 30, the high level of DMN functional connectivity on Day 1

seems to reflect the increase of alert level in monitoring further external stimuli [31], or the shifts of axonal ion and neurotransmitters of the neurons as suggested in animal studies [47]. The normal connectivity seems to be disrupted and the functional connectivity of DMN is significantly reduced on Day 7, compared to Day 1. Although we do not have data comparing neurophysiology to the functional connectivity modification observed, animal models demonstrate the cyclical changes of axonal ion distribution and neurotransmitters within the first few days of a concussion [47]. The lack of noticeable change in structural connectivity and gross anatomy confirmed that the concussions in our athletes did not lead to severe anatomical damage.

Our concussed subjects demonstrated a significantly reduced DMN functional connectivity on Day 7, compared to the control subjects. This finding is consistent with the prior findings from Johnson et al. [14], who collected rs-fMRI data around 10 days after concussion, and from Mayer et al. [17], who collected rs-fMRI data around 11.5 days after concussion. Mayer et al. did not find change in functional connectivity across a 4-month recovery period. We observed a trend (but not statistically significant) of recovery of DMN functional connectivity from Day 7 to Day 30. While the observation is different between our and Mayer's groups, the consistent view is that the recovery process is slow from Day 7 to Day 30, compared to the rapid reduction of DMN functional connectivity from Day 1 to Day 7.

Compared to the control group, the mean DMN overall connectivity of concussed group was higher by 14.5% on Day 1, but lower by 41.4% on Day 7 (significant with a large effect size of 1.51 in Hedges' g), and then recovered but still lower by 15% on Day 30. However, we did not find significant difference on DMN functional connectivity between the control group and Day 1 or Day 30 after concussion with the concussed group, probably due to inter-subject

variation and a relatively small sample size. Considering the significantly reduced cognitive ability as demonstrated by neuropsychological tests on Day 1 after concussion, it is reasonable to speculate that there was an abnormally increased level of DMN functional connectivity, followed by a severe significant reduction and then a slow recovery. The control group was composed of non-athlete college students, although they were physically active. It is possible that the control group did not fully represent the neuronal characteristics of the non-concussed athletes. Comparing with a control group composed of student-athletes from non-contact sports and collecting rs-fMRI data at baseline (before concussion) will be worthwhile to further our understanding of the true state after concussion. We have started collecting baseline MRI data, along with baseline ImPACT data, from student-athletes when they start their freshman year with no known prior concussions. When a concussion occurs in these athletes, we will collect MRI and ImPACT data within the 24 hours, and on Days 7, 30 and 90 to track the recovery process.

We did not find significant change of structural connectivity between ICCs and other regions of the DMN after concussion. Although the FA of the full skeleton was noted statistically significantly reduced from Day 1 to Day 30 after concussion, the change was only 2%. This is very small compared to the functional connectivity change in the range of 15-40% that was found. The changes after concussion on corpus callosum and on cingulum were not significant, and the mean FA changes were less than 2.2%. We did not find significant changes on other diffusion metrics MD, AD and RD on the skeleton generated from TBSS. Although the sample size is relatively small, the structural connectivity and TBSS results suggest that the structural connectivity is relatively stable or the alteration is very subtle within DMN after concussion. Some prior DTI studies have found significant change in the white matter, but with some variations. Mayer et al. [22] found significantly greater fractional anisotropy (FA) in corpus

callosum (CC) and several tracts in the left hemisphere. On the other hand, the meta-analysis performed by Aoki et al. [23] on DTI of mTBI demonstrated significant reduction of FA and significant increase of mean diffusivity (MD) in CC, a region likely prone to shear strain during physical impact. The reduction of FA suggests the reduction of axonal integrity. Since CC connects the two hemispheres, the axonal damage on CC would likely impact the DMN, which distributes in both hemispheres and various lobes of the brain, and thus reduces the DMN functional connectivity, as shown in our results. However, consistent with our finding, Maguans et al. did not find alteration in the diffusion metrics and brain anatomy < 72 hours, 14 days and > 30 days after sported-related concussion in 12 subjects (age 11-15). They did not find difference in the diffusion metrics compared to their control group either [48]. Thus, the findings heavily depend on the concussion population and the methods applied.

Resting-state fMRI is still a technique under development, with some limitation in reproducibility at the individual level [49]. We designed a protocol with two 7-minute scans to improve the reproducibility of the technique, by reducing the effects of random noise and uncorrelated brain activity. In rs-fMRI data analyses, global signal regression has been commonly modeled as a nuisance physiological signal and is removed in the pre-processing steps. We have also applied the global signal regression in this work. As discussed in the work by Murphy et al.[50], the global signal regression could create negatively correlated regions in the brain. In our work, the focus is on the DMN. The potential negatively correlated regions due to the global signal regression would not change the findings. There are some potential benefits in applying global signal regression in this study. After a concussion, the global cerebral blood flow might change. The global signal regression can be helpful in reducing the difference in the global cerebral blood flow to uncover the true neuronal functional connectivity. We also re-analyzed

our concussed data without global signal regression in the pre-processing step. As expected, the mean correlation to each node and the overall DMN correlation in each time point were elevated. The significant drop on Day 7 compared to Day 1 on the DMN after concussion was still found. The recovery trend from Day 7 to Day 30 maintained also. Successful tractography based on DTI data also faces some fundamentally challenging demands, specifically the need of high image signal-to-noise ratio, high spatial resolution, the ability to resolve crossing fibers, full coverage of tracks of interest, and the ability to track at regions with low anisotropy [49]. Thus, we limited the investigation of the structural connectivity at the cingulum, which links the PCC and the prefrontal regions.

In the current study, within the first 24 hours after concussion we typically documented an abnormal clinical exam and ImPACT scores, but both typically returned to normal within 7 days. The structural MRI and DTI appeared stable on the three time points. Clinical abnormality was found in only one case, which was likely a pre-existing condition, because the abnormality appeared stable over 30 days. One normal subject also demonstrated a pre-existing brain abnormality that was also stable over 30 days. In addition to the DTI findings discussed above, these findings imply that in a typical sports-related concussion there is no significant edema or major axonal tract damage. These observations also indicate that the short-term clinical response to mTBI is excellent despite the abnormal DMN functional connectivity on Day 7. However, larger studies are needed to validate these finding and more importantly to investigate longer-term issues from mTBI as outlined below.

Giza[47] and Harris[51] have outlined nicely the profound physiologic cascade following an mTBI in animal models. Interestingly, glucose metabolism increases initially, but is followed by a hypo-metabolic state. There is abnormality with glutamate and NMDA receptors along with

pathophysiologic changes in brain metabolism. Elevations in calcium (which can affect mitochondrial function) can remain abnormal for three weeks or longer. All of these metabolic related derangements typically returned to normal without significant anatomic or long-term clinical changes. Our rs-fMRI results in mTBI mirrors the results of these animal studies. A hyper-connectivity (although not significant) was noted within the first 24 hours, followed by a significantly reduced functional connectivity on Day 7, and then an improved but not quite normal functional connectivity on Day 30. The acquired clinical MRI and DTI at the same time points appeared relatively stable. The initial clinical examination and ImPACT scores typically showed full recovery within seven days. These data imply that the DMN functional connectivity measured with rs-fMRI better reflects the recovery of the underlying neurophysiology than routine clinical MRI, DTI, ImPACT and neurologic examination.

A clinical condition known as "second impact syndrome" [52] is also important to discuss. In this syndrome, an additional concussion, typically soon after the first one and apparently before the brain pathophysiology converts to normal, may cause a cascade of neuro-metabolic events that can be far more dangerous clinically than a typical sports-related concussion [47]. Therefore, athletes traditionally are required to avoid contact until the clinical examination and ImPACT tests demonstrate a full recovery. The typical time has been three to seven days. However, a longer recovery time (as long as a month) may be needed as demonstrated by DMN functional connectivity. Our data imply that normal neurologic examination and ImPACT scores might not be sufficient to assure full neurophysiologic recovery from mTBI. This is important to consider as clinicians wish to reduce danger from a "second impact syndrome" in a “partially” recovered brain. Further studies are needed to confirm this. The potential additive effect of many mTBI over time with or without second impact events (chronic traumatic encephalopathy (CTE)) has

been implied elsewhere [53]. The current study does not confirm the presence of CTE. In our study, the athlete with a repeated concussion suffered the second concussion more than two months after the first one. Full recovery was expected before the second incidence. Properly powered longitudinal studies will be needed to fully evaluate this clinical concept. However, advanced imaging techniques like rs-fMRI may help document full brain healing prior to returning a student-athlete to play.

The rs-fMRI finding in this study may imply that the total human physiologic recovery from mTBI may actually be longer than previously thought and is difficult to assess with standard clinical examination and ImPACT testing alone. If this is confirmed with additional, broader clinical trials, routine clinical exam and computer assisted neuro-psychological tests may not be sufficient to determine safe return to play given the concept of second impact syndrome and CTE noted above.

In conclusion, we demonstrated that it is possible to perform a longitudinal MR neuroimaging study starting on Day 1 post concussion to track the alteration of functional and structural connectivity over a month on Division 1 collegiate football student-athletes in season. There is a significant dynamic modification of DMN connectivity during the first 7 days post concussion. The results imply the importance of imaging the brain in early acute phase post concussion. We also successfully tested our hypothesis that the functional connectivity of the DMN would dynamically change over the course of recovery after concussion, but the structural connectivity of the DMN and anatomical structure would remain relatively stable. In this small pilot study, the network-based and seed-based whole-brain functional connectivity analyses both demonstrated that the functional connectivity of DMN measured with longitudinal rs-fMRI can

serve as a potential biomarker to monitor the dynamically changing brain function after sports-related concussion.

**Acknowledgements**

The authors thank suggestions from Drs. Erik Shapiro and Eric Eggenberger, concussed subject assessment assistance from Drs. Albert Aniskiewicz, Michael Shingles, Douglas Dietzel and Michael Andary, and support from Head Football Coach Mr. Mark Dantonio at Michigan State University. This work was supported by the Michigan State University Radiology Pilot Scan Program.

**Author Disclosure Statement**

No competing financial interests exist.

## References

1. Langlois, J.A., Rutland-Brown, W. and Wald, M.M. (2006). The epidemiology and impact of traumatic brain injury: a brief overview. J Head Trauma Rehabil 21, 375-378.

2. Ruff, R.M. (2011). Mild traumatic brain injury and neural recovery: rethinking the debate. NeuroRehabilitation 28, 167-180.

3. Giza, C.C., Kutcher, J.S., Ashwal, S., Barth, J., Getchius, T.S., Gioia, G.A., Gronseth, G.S., Guskiewicz, K., Mandel, S., Manley, G., McKeag, D.B., Thurman, D.J. and Zafonte, R. (2013). Summary of evidence-based guideline update: Evaluation and management of concussion in sports: Report of the Guideline Development Subcommittee of the American Academy of Neurology. Neurology.

4. Mayers, L.B. and Redick, T.S. (2012). Clinical utility of ImPACT assessment for postconcussion return-to-play counseling: psychometric issues. J Clin Exp Neuropsychol 34, 235-242.

5. McCrea, M., Guskiewicz, K., Randolph, C., Barr, W.B., Hammeke, T.A., Marshall, S.W. and Kelly, J.P. (2009). Effects of a symptom-free waiting period on clinical outcome and risk of reinjury after sport-related concussion. Neurosurgery 65, 876-882; discussion 882-873.

6. McCrea, M., Guskiewicz, K.M., Marshall, S.W., Barr, W., Randolph, C., Cantu, R.C., Onate, J.A., Yang, J. and Kelly, J.P. (2003). Acute effects and recovery time following concussion in collegiate football players: the NCAA Concussion Study. JAMA 290, 2556-2563.

7. Lau, B.C., Kontos, A.P., Collins, M.W., Mucha, A. and Lovell, M.R. (2011). Which on-field signs/symptoms predict protracted recovery from sport-related concussion among high school football players? Am J Sports Med 39, 2311-2318.

8. Fox, M.D. and Raichle, M.E. (2007). Spontaneous fluctuations in brain activity observed with functional magnetic resonance imaging. Nat Rev Neurosci 8, 700-711.

9. Basser, P.J., Pajevic, S., Pierpaoli, C., Duda, J. and Aldroubi, A. (2000). In vivo fiber tractography using DT-MRI data. Magn Reson Med 44, 625-632.

10. Behrens, T.E., Berg, H.J., Jbabdi, S., Rushworth, M.F. and Woolrich, M.W. (2007). Probabilistic diffusion tractography with multiple fibre orientations: What can we gain? Neuroimage 34, 144-155.

11. Le Bihan, D., Mangin, J.F., Poupon, C., Clark, C.A., Pappata, S., Molko, N. and Chabriat, H. (2001). Diffusion tensor imaging: concepts and applications. J Magn Reson Imaging 13, 534-546.

12. Guskiewicz, K.M., Weaver, N.L., Padua, D.A. and Garrett, W.E., Jr. (2000). Epidemiology of concussion in collegiate and high school football players. Am J Sports Med 28, 643-650.

13. Raichle, M.E. and Mintun, M.A. (2006). Brain work and brain imaging. Annu Rev Neurosci 29, 449-476.

14. Johnson, B., Zhang, K., Gay, M., Horovitz, S., Hallett, M., Sebastianelli, W. and Slobounov, S. (2012). Alteration of brain default network in subacute phase of injury in concussed individuals: resting-state fMRI study. Neuroimage 59, 511-518.

15. Slobounov, S.M., Gay, M., Zhang, K., Johnson, B., Pennell, D., Sebastianelli, W., Horovitz, S. and Hallett, M. (2011). Alteration of brain functional network at rest and in response to YMCA physical stress test in concussed athletes: RsFMRI study. Neuroimage 55, 1716-1727.

16. Zhang, K., Johnson, B., Gay, M., Horovitz, S.G., Hallett, M., Sebastianelli, W. and Slobounov, S. (2012). Default mode network in concussed individuals in response to the YMCA physical stress test. J Neurotrauma 29, 756-765.

17. Mayer, A.R., Mannell, M.V., Ling, J., Gasparovic, C. and Yeo, R.A. (2011). Functional connectivity in mild traumatic brain injury. Hum Brain Mapp 32, 1825-1835.

18. Zhou, Y., Milham, M.P., Lui, Y.W., Miles, L., Reaume, J., Sodickson, D.K., Grossman, R.I. and Ge, Y. (2012). Default-mode network disruption in mild traumatic brain injury. Radiology 265, 882-892.

19. Shumskaya, E., Andriessen, T.M., Norris, D.G. and Vos, P.E. (2012). Abnormal whole-brain functional networks in homogeneous acute mild traumatic brain injury. Neurology 79, 175-182.

20. Messe, A., Caplain, S., Pelegrini-Issac, M., Blancho, S., Levy, R., Aghakhani, N., Montreuil, M., Benali, H. and Lehericy, S. (2013). Specific and evolving resting-state network alterations in post-concussion syndrome following mild traumatic brain injury. PLoS One 8, e65470.

21. Han, K., Mac Donald, C.L., Johnson, A.M., Barnes, Y., Wierzechowski, L., Zonies, D., Oh, J., Flaherty, S., Fang, R., Raichle, M.E. and Brody, D.L. (2014). Disrupted modular organization of resting-state cortical functional connectivity in U.S. military personnel following concussive 'mild' blast-related traumatic brain injury. Neuroimage 84, 76-96.

22. Mayer, A.R., Ling, J., Mannell, M.V., Gasparovic, C., Phillips, J.P., Doezema, D., Reichard, R. and Yeo, R.A. (2010). A prospective diffusion tensor imaging study in mild traumatic brain injury. Neurology 74, 643-650.

23. Aoki, Y., Inokuchi, R., Gunshin, M., Yahagi, N. and Suwa, H. (2012). Diffusion tensor imaging studies of mild traumatic brain injury: a meta-analysis. J Neurol Neurosurg Psychiatry 83, 870-876.

24. Zhang, K., Johnson, B., Pennell, D., Ray, W., Sebastianelli, W. and Slobounov, S. (2010). Are functional deficits in concussed individuals consistent with white matter structural alterations: combined FMRI & DTI study. Exp Brain Res 204, 57-70.

25. Zhu, D.C., Majumdar, S., Korolev, I.O., Berger, K.L. and Bozoki, A.C. (2013). Alzheimer's disease and amnestic mild cognitive impairment weaken connections within the default-mode network: a multi-modal imaging study. J Alzheimers Dis 34, 969-984.

26. Raichle, M.E., MacLeod, A.M., Snyder, A.Z., Powers, W.J., Gusnard, D.A. and Shulman, G.L. (2001). A default mode of brain function. Proc Natl Acad Sci U S A 98, 676-682.

27. Greicius, M.D., Srivastava, G., Reiss, A.L. and Menon, V. (2004). Default-mode network activity distinguishes Alzheimer's disease from healthy aging: evidence from functional MRI. Proc Natl Acad Sci U S A 101, 4637-4642.

28. Greicius, M.D., Supekar, K., Menon, V. and Dougherty, R.F. (2009). Resting-state functional connectivity reflects structural connectivity in the default mode network. Cereb Cortex 19, 72-78.

29. Supekar, K., Menon, V., Rubin, D., Musen, M. and Greicius, M.D. (2008). Network analysis of intrinsic functional brain connectivity in Alzheimer's disease. PLoS Comput Biol 4, e1000100.

30. Zhang, H.Y., Wang, S.J., Liu, B., Ma, Z.L., Yang, M., Zhang, Z.J. and Teng, G.J. (2010). Resting brain connectivity: changes during the progress of Alzheimer disease. Radiology 256, 598-606.

31. Buckner, R.L., Andrews-Hanna, J.R. and Schacter, D.L. (2008). The brain's default network: anatomy, function, and relevance to disease. Ann N Y Acad Sci 1124, 1-38.

32. Woolsey, T.A., Hanaway, J. and Gado, M.H. (2003). The brain atlas: a visual guide to the human central nervous system. 2nd ed. John Wiley & Sons, Inc.: Hoboken, New Jersey.

33. Iverson, G.L., Lovell, M.R. and Collins, M.W. (2005). Validity of ImPACT for measuring processing speed following sports-related concussion. J Clin Exp Neuropsychol 27, 683-689.

34. Schatz, P. (2010). Long-term test-retest reliability of baseline cognitive assessments using ImPACT. Am J Sports Med 38, 47-53.

35. Schatz, P., Pardini, J.E., Lovell, M.R., Collins, M.W. and Podell, K. (2006). Sensitivity and specificity of the ImPACT Test Battery for concussion in athletes. Arch Clin Neuropsychol 21, 91-99.

36. Schatz, P. and Sandel, N. (2013). Sensitivity and specificity of the online version of ImPACT in high school and collegiate athletes. Am J Sports Med 41, 321-326.

37. McCrory, P., Meeuwisse, W., Aubry, M. and al., e. (2013). Consensus statement on concussion in sport: the 4th International Conference on Concussion in Sport held in Zurich, November 2012 BJSM online 47, 250-258.

38. Smith, S.M., Jenkinson, M., Woolrich, M.W., Beckmann, C.F., Behrens, T.E., Johansen-Berg, H., Bannister, P.R., De Luca, M., Drobnjak, I., Flitney, D.E., Niazy, R.K., Saunders, J., Vickers, J., Zhang, Y., De Stefano, N., Brady, J.M. and Matthews, P.M. (2004). Advances in functional and structural MR image analysis and implementation as FSL. Neuroimage 23 Suppl 1, S208-219.

39. Cox, R.W. (1996). AFNI: software for analysis and visualization of functional magnetic resonance neuroimages. Comput Biomed Res 29, 162-173.

40. Ward, B. (2000). Deconvolution analysis of fMRI time series Data: Milwaukee.

41. Fischl, B., Salat, D.H., Busa, E., Albert, M., Dieterich, M., Haselgrove, C., van der Kouwe, A., Killiany, R., Kennedy, D., Klaveness, S., Montillo, A., Makris, N., Rosen, B. and Dale, A.M. (2002). Whole brain segmentation: automated labeling of neuroanatomical structures in the human brain. Neuron 33, 341-355.

42. Fox, M.D., Snyder, A.Z., Vincent, J.L., Corbetta, M., Van Essen, D.C. and Raichle, M.E. (2005). The human brain is intrinsically organized into dynamic, anticorrelated functional networks. Proc Natl Acad Sci U S A 102, 9673-9678.

43. Yeo, B.T., Krienen, F.M., Sepulcre, J., Sabuncu, M.R., Lashkari, D., Hollinshead, M., Roffman, J.L., Smoller, J.W., Zollei, L., Polimeni, J.R., Fischl, B., Liu, H. and Buckner, R.L. (2011). The organization of the human cerebral cortex estimated by intrinsic functional connectivity. J Neurophysiol 106, 1125-1165.

44. Ward, B. (2000). Simultaneous inference for fMRI data: Milwaukee.

45. Behrens, T.E., Woolrich, M.W., Jenkinson, M., Johansen-Berg, H., Nunes, R.G., Clare, S., Matthews, P.M., Brady, J.M. and Smith, S.M. (2003). Characterization and propagation of uncertainty in diffusion-weighted MR imaging. Magn Reson Med 50, 1077-1088.

46. Mori, S., Oishi, K., Jiang, H., Jiang, L., Li, X., Akhter, K., Hua, K., Faria, A.V., Mahmood, A., Woods, R., Toga, A.W., Pike, G.B., Neto, P.R., Evans, A., Zhang, J., Huang, H., Miller, M.I., van Zijl, P. and Mazziotta, J. (2008). Stereotaxic white matter atlas based on diffusion tensor imaging in an ICBM template. Neuroimage 40, 570-582.

47. Giza, C.C. and Hovda, D.A. (2001). The Neurometabolic Cascade of Concussion. J Athl Train 36, 228-235.

48. Maugans, T.A., Farley, C., Altaye, M., Leach, J. and Cecil, K.M. (2012). Pediatric sports-related concussion produces cerebral blood flow alterations. Pediatrics 129, 28-37.

49. Zhu, D.C. and Majumdar, S. (2014). Integration of resting-state FMRI and diffusion-weighted MRI connectivity analyses of the human brain: limitations and improvement. J Neuroimaging 24, 176-186.

50. Murphy, K., Birn, R.M., Handwerker, D.A., Jones, T.B. and Bandettini, P.A. (2009). The impact of global signal regression on resting state correlations: are anti-correlated networks introduced? Neuroimage 44, 893-905.

51. Harris, J.L., Yeh, H.W., Choi, I.Y., Lee, P., Berman, N.E., Swerdlow, R.H., Craciunas, S.C. and Brooks, W.M. (2012). Altered neurochemical profile after traumatic brain injury: (1)H-MRS biomarkers of pathological mechanisms. J Cereb Blood Flow Metab 32, 2122-2134.

52. Bey, T. and Ostick, B. (2009). Second impact syndrome. West J Emerg Med 10, 6-10.

53. McKee, A.C., Cantu, R.C., Nowinski, C.J., Hedley-Whyte, E.T., Gavett, B.E., Budson, A.E., Santini, V.E., Lee, H.S., Kubilus, C.A. and Stern, R.A. (2009). Chronic traumatic encephalopathy in athletes: progressive tauopathy after repetitive head injury. J Neuropathol Exp Neurol 68, 709-735.

## Figure Legends

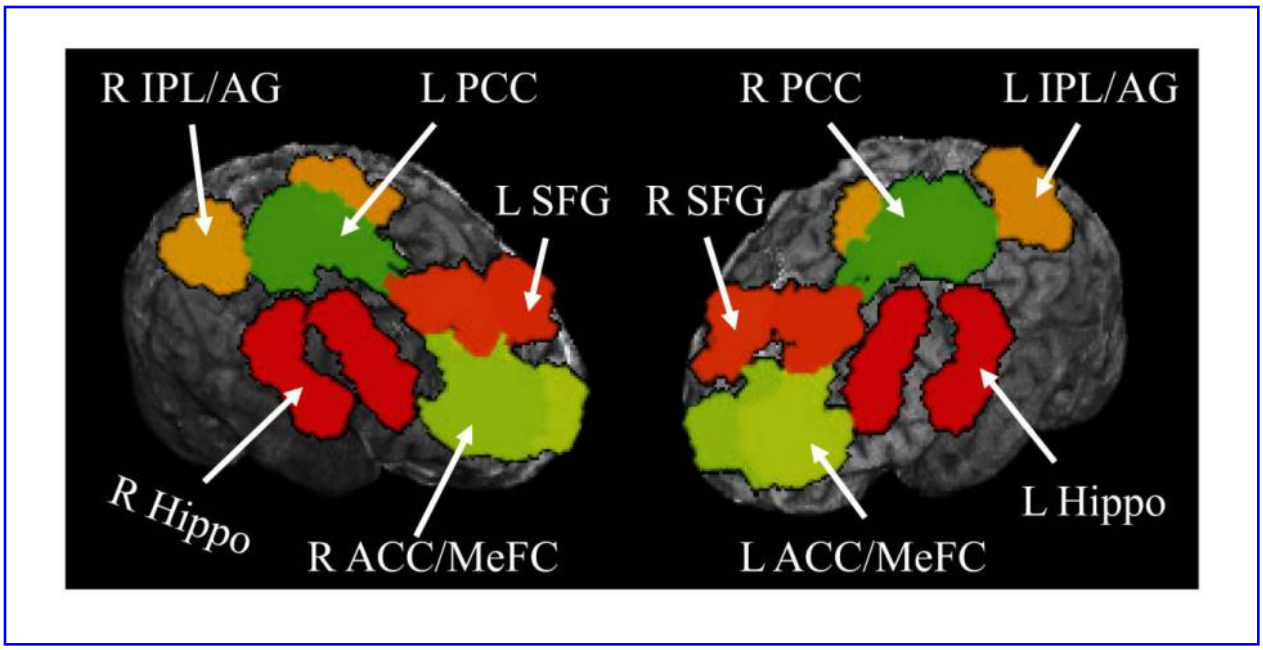


Fig. 1. The nodes (in color)used in the DMN network-based analyses are shown on one of our subjects. PCC = posterior cingulate cortex, ACC = anterior cingulate cortex, MeFC = medial frontal cortex, SFG = superior frontal gyrus, IPL = inferior parietal lobule, AG = angular gyrus, Hippo = hippocampus, DMN = default-mode network, R = right, L = left.

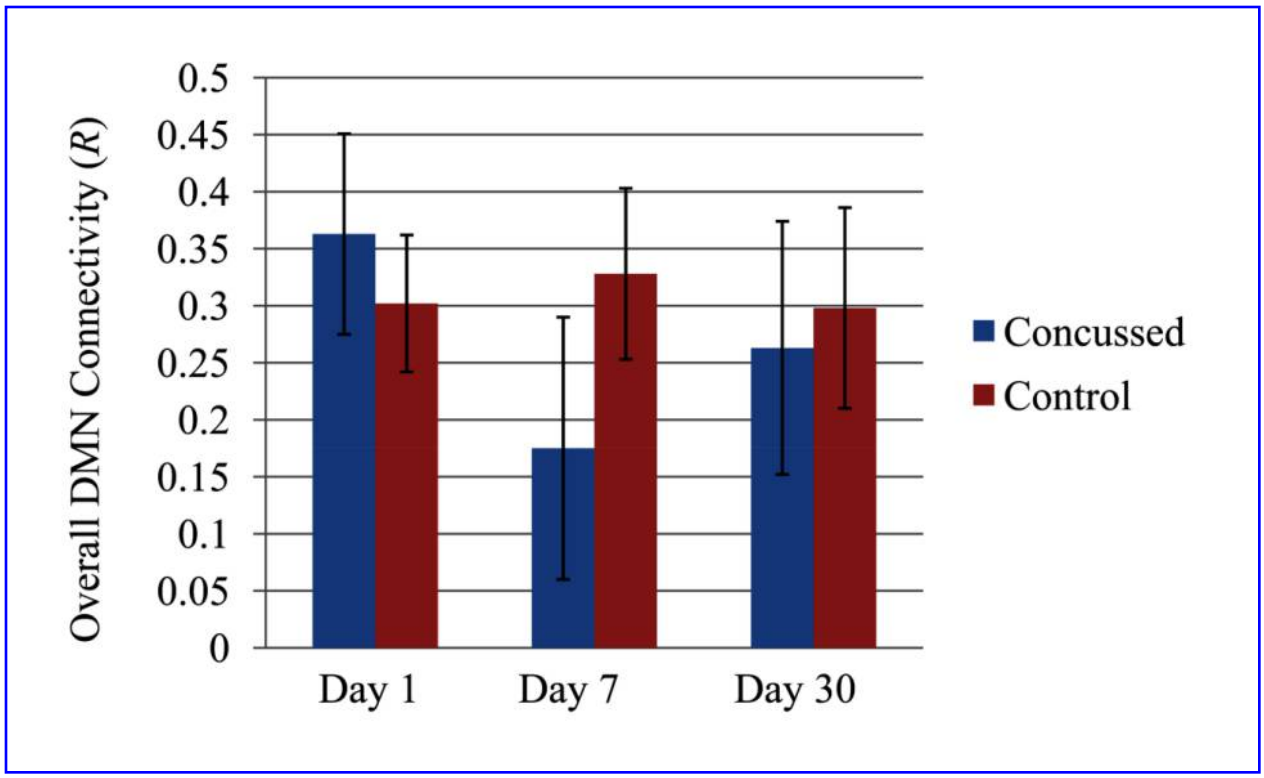


Fig. 2. The overall DMN functional connectivity (in mean ± standard deviation of correlation coefficient *R*) is shown for the 7 concussed and 11 control subjects.

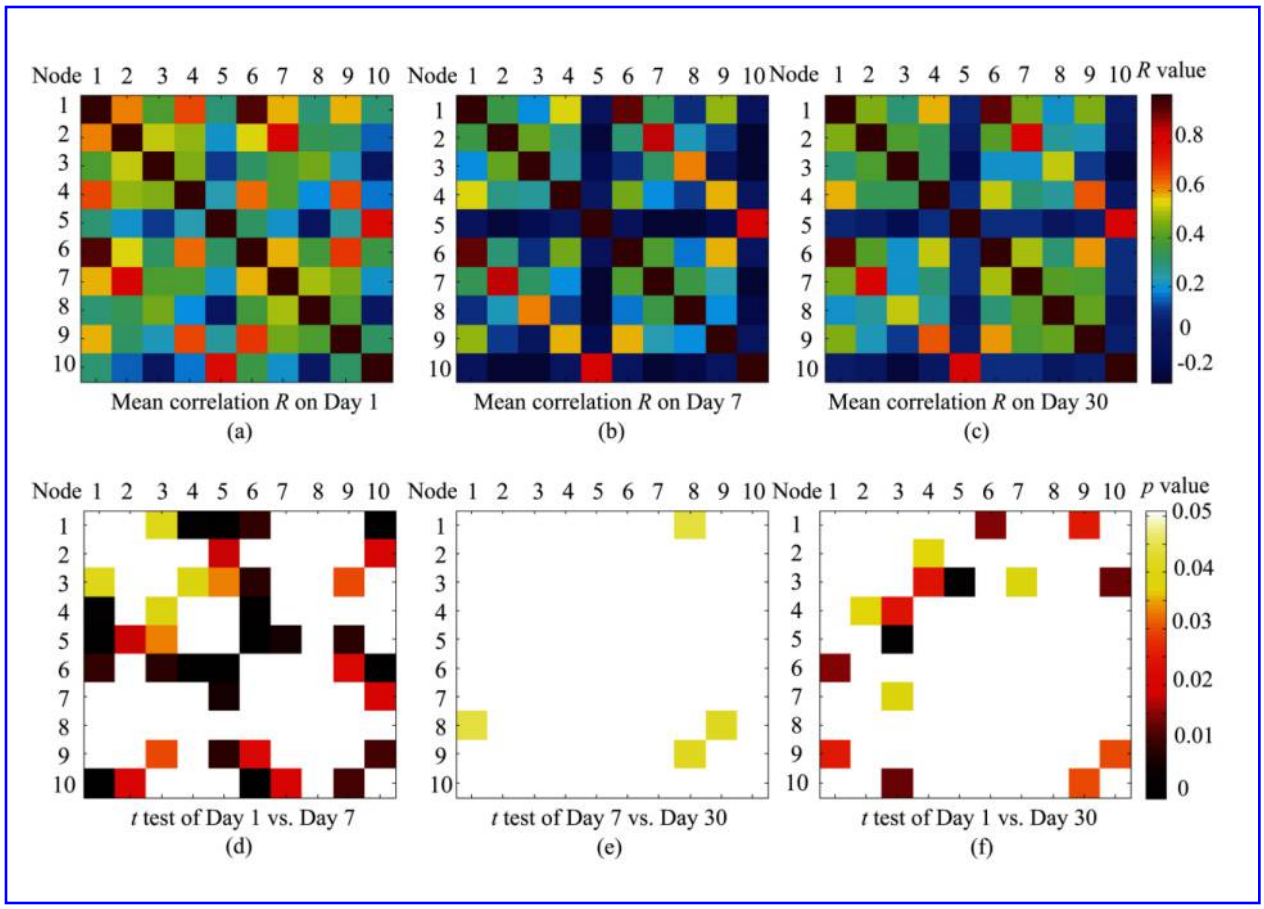


Fig. 3. The functional connectivity (mean correlation *R*) between each pair of nodes within the default-mode network after concussion (n = 7) on (a) Day 1, (b) Day 7, and (c) Day 30 is shown. The 2-tail paired *t* test results (in color) are shown for (d) Day 1 vs. Day 7, (e) Day 7 vs. Day 30, and (f) Day 1 vs. Day 30 on each pair of nodes. Only $p < 0.05$ (in color) is shown. Node 1 = left PCC, 2 = left ACC/MeFC, 3 = left SFG, 4 = left IPL/AG, 5 = left hippocampus, 6 = right PCC, 7 = right ACC/MeFC, 8 = right SFG, 9 = right IPL/AG, 10 = right hippocampus.

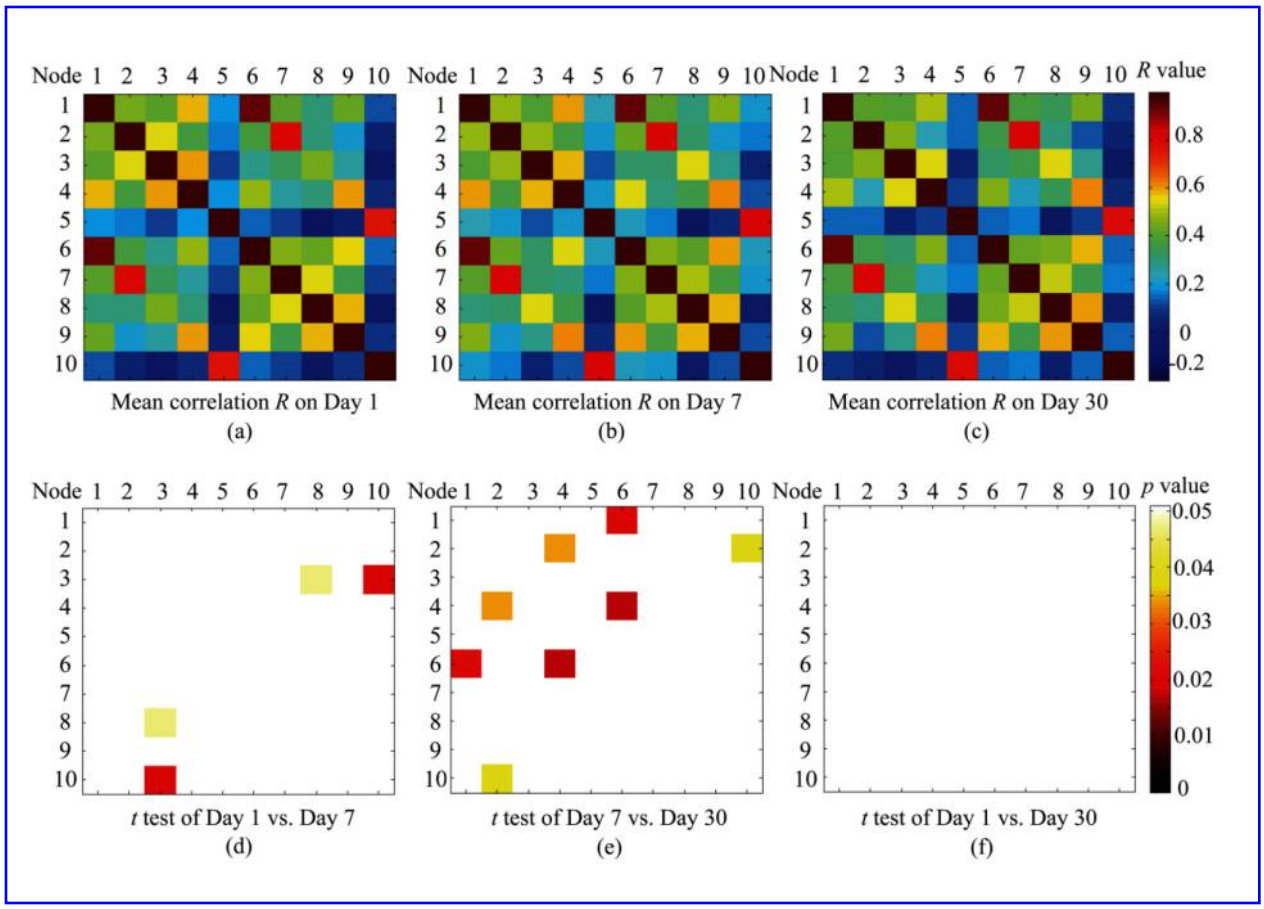


Fig. 4. The functional connectivity (mean correlation *R*) between each pair of nodes within the default-mode network of control subjects on (a) Day 1, (b) Day 7, and (c) Day 30 is shown. The 2-tail paired *t* test results (in color) are shown comparing (d) Day 1 vs. Day 7, (e) Day 7 vs. Day 30, and (f) Day 1 vs. Day 30 on each pair of nodes. Only $p < 0.05$ (in color) is shown.

Node 1 = left PCC, 2 = left ACC/MeFC, 3 = left SFG, 4 = left IPL/AG, 5 = left hippocampus, 6 = right PCC, 7 = right ACC/MeFC, 8 = right SFG, 9 = right IPL/AG, 10 = right hippocampus.

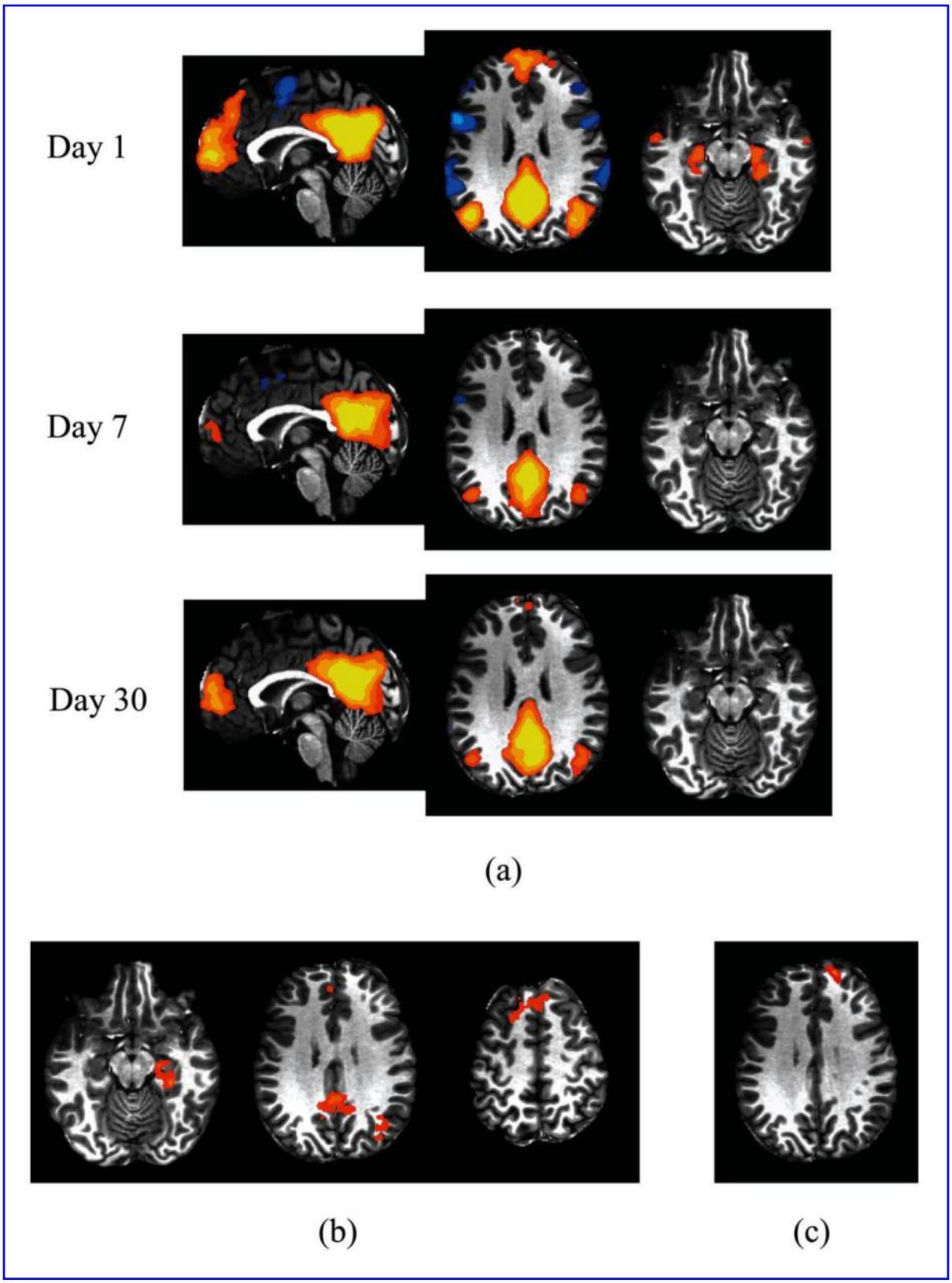

Fig. 5. Shown are (a) the mean functional connectivity to left isthmus of cingulate cortex (ICC) of the concussed group (correlation $R > 0.25$, n = 7), (b) ANOVA results of Day 1 vs. Day 7 (n = 8), and (c) ANOVA results of Day 1 vs. Day 30 (n = 7). The significant clusters of Day 1 > Day 7 (b) and Day 1 > Day 30 (c) are shown in red/yellow color.

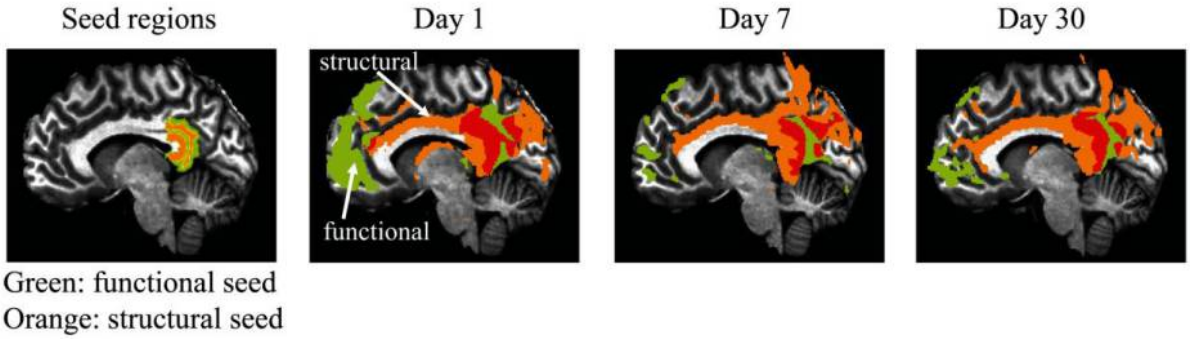


Fig. 6. Case study: The functional (in green and red) and structural (in orange and red) connectivity to left isthmus of cingulate cortex of a concussed subject over one month (correlation $R > 0.4$ and connectivity distribution > 1000). Red: overlap regions.

Table 1. ImPACT composite scores of concussed athletes

| | | Mean | STD | p value+ |
|---|---|---|---|---|
| Baseline | Verbal memory composite | 79.0 | 13.7 | - |
| | Visual memory composite | 71.8 | 14.6 | - |
| | Motor processing speed composite | 41.5 | 4.4 | - |
| | Reaction time composite | 0.581 | 0.058 | - |
| | Impulse control composite | 7.88 | 7.36 | - |
| | Total symptom score | 5.5 | 11.5 | - |
| Day 1 | Verbal memory composite | 66.9 | 23.9 | 0.049* |
| | Visual memory composite | 56.6 | 23.1 | 0.007* |
| | Motor processing speed composite | 34.0 | 9.7 | 0.004* |
| | Reaction time composite | 0.718 | 0.160 | 0.009* |
| | Impulse control composite | 6.88 | 6.29 | 0.741 |
| | Total symptom score | 27.8 | 15.8 | 0.003* |
| Day 7 | Actual Day Tested | 6.0 | 2.4 | |
| | Verbal memory composite | 87.3 | 10.7 | 0.195 |
| | Visual memory composite | 82.9 | 14.2 | 0.020** |
| | Motor processing speed composite | 41.4 | 5.9 | 0.739 |
| | Reaction time composite | 0.605 | 0.100 | 0.625 |
| | Impulse control composite | 7.38 | 4.90 | 0.844 |
| | Total symptom score | 2.8 | 4.0 | 0.544 |

STD: Standard deviation

+ANOVA Pair-wise comparisons versus baseline test scores.
*significantly worse than baseline, ** significantly better than baseline

Table 2. The connectivity to each node from rest of DMN and the overall DMN connectivity Days 1 to 30 after concussion

| Days | ROI name | L PCC | L ACC/ MeFC | L SFG | L IPL/AG | L Hipp | R PCC | R ACC/ MeFC | R SFG | R IPL/AG | R Hipp | Overall DMN |
|---|---|---|---|---|---|---|---|---|---|---|---|---|
| Day 1$^{+}$ | mean of *R* | 0.515 | 0.450 | 0.308 | 0.424 | 0.239 | 0.520 | 0.458 | 0.284 | 0.424 | 0.223 | 0.354 |
| | STD of *R* | 0.065 | 0.104 | 0.130 | 0.132 | 0.125 | 0.078 | 0.076 | 0.117 | 0.108 | 0.151 | 0.085 |
| Day 7$^{+}$ | mean of *R* | 0.317 | 0.253 | 0.174 | 0.254 | 0.007 | 0.311 | 0.269 | 0.159 | 0.221 | 0.001 | 0.181 |
| | STD of *R* | 0.146 | 0.161 | 0.127 | 0.098 | 0.140 | 0.138 | 0.168 | 0.090 | 0.074 | 0.146 | 0.108 |
| Day 30$^{++}$ | mean of *R* | 0.386 | 0.330 | 0.198 | 0.342 | 0.126 | 0.405 | 0.364 | 0.263 | 0.328 | 0.107 | 0.263 |
| | STD of *R* | 0.150 | 0.126 | 0.145 | 0.131 | 0.157 | 0.150 | 0.152 | 0.117 | 0.112 | 0.124 | 0.111 |
| ANOVA$^{++}$ | *P* value | 0.010 | 0.023 | 0.012 | 0.010 | 0.007 | 0.007 | 0.055 | 0.030 | 0.009 | 0.010 | 0.006 |
| | *F* statistics | 6.981 | 5.292 | 6.536 | 6.935 | 7.832 | 7.636 | 3.720 | 4.783 | 7.282 | 6.920 | 7.956 |
| Day 1 vs. Day 7$^{+}$ | *p* value | 0.005* | 0.016 | 0.011 | 0.007 | 0.008 | 0.002* | 0.029 | 0.014 | 0.007 | 0.013 | 0.005* |
| | *t* statistics | 4.03 | 3.18 | 3.46 | 3.78 | 3.69 | 4.82 | 2.74 | 3.26 | 3.74 | 3.29 | 4.08 |
| | Hedges' g | 1.739 | 1.388 | 0.992 | 1.377 | 1.645 | 1.819 | 1.422 | 1.136 | 1.996 | 1.407 | 1.695 |
| Day 7 vs. Day 30$^{++}$ | *p* value | 0.292 | 0.244 | 0.569 | 0.177 | 0.167 | 0.191 | 0.260 | 0.022 | 0.101 | 0.206 | 0.156 |
| | *t* statistics | -1.16 | -1.29 | -0.60 | -1.53 | -1.57 | -1.47 | -1.24 | -3.07 | -1.93 | -1.42 | -1.62 |
| | Hedges' g | -0.490 | -0.567 | -0.162 | -0.658 | -0.878 | -0.656 | -0.626 | -0.939 | -1.046 | -0.811 | -0.741 |
| Day 1 vs. Day 30$^{++}$ | *p* value | 0.041 | 0.068 | 0.036 | 0.048 | 0.084 | 0.074 | 0.152 | 0.740 | 0.072 | 0.078 | 0.053 |
| | *t* statistics | 2.59 | 2.22 | 2.70 | 2.47 | 2.07 | 2.16 | 1.64 | 0.35 | 2.18 | 2.13 | 2.41 |
| | Hedges' g | 1.140 | 0.942 | 0.795 | 0.698 | 0.959 | 1.018 | 0.765 | 0.131 | 0.865 | 1.044 | 0.955 |

*R* = correlation coefficient, STD = standard deviation, L = left, R = right

PCC = posterior cingulate cortex, ACC = anterior cingulate cortex, MeFC = medial frontal cortex, SFG = superior frontal gyrus
IPL = inferior parietal lobule, AG = angular gyrus, Hipp = hippocampus, DMN = default-mode network.
$^{+}$Based on all 8 subjects. $^{++}$Based on 7 subjects after removing the one without Day 30 data.

2-tail paired *t* tests were performed in all paired wise comparison.
To account for Bonferroni correction, thresholds of significance: $p \leq 0.0052$ for overall DMN, $p \leq 0.005$ for each node.
*indicates statistically significant.

Table 3. The connectivity to each node from rest of DMN and the overall DMN connectivity Days 1 to 30 for healthy controls

| Days | ROI name | L PCC | L ACC/ MeFC | L SFG | L IPL/AG | L Hipp | R PCC | R ACC/ MeFC | R SFG | R IPL/AG | R Hipp | Overall DMN |
|---|---|---|---|---|---|---|---|---|---|---|---|---|
| Day 1 | mean of *R* | 0.426 | 0.363 | 0.326 | 0.384 | 0.185 | 0.424 | 0.376 | 0.313 | 0.346 | 0.144 | 0.302 |
| | STD of *R* | 0.060 | 0.097 | 0.116 | 0.103 | 0.046 | 0.062 | 0.087 | 0.104 | 0.094 | 0.064 | 0.060 |
| Day 7 | mean of *R* | 0.448 | 0.385 | 0.344 | 0.410 | 0.220 | 0.459 | 0.395 | 0.326 | 0.368 | 0.215 | 0.328 |
| | STD of *R* | 0.094 | 0.099 | 0.106 | 0.092 | 0.100 | 0.082 | 0.100 | 0.096 | 0.075 | 0.100 | 0.075 |
| Day 30 | mean of *R* | 0.403 | 0.325 | 0.325 | 0.342 | 0.180 | 0.424 | 0.379 | 0.342 | 0.362 | 0.167 | 0.298 |
| | STD of *R* | 0.112 | 0.132 | 0.103 | 0.097 | 0.111 | 0.110 | 0.115 | 0.102 | 0.107 | 0.106 | 0.088 |
| ANOVA | *p* value | 0.403 | 0.226 | 0.854 | 0.111 | 0.475 | 0.415 | 0.817 | 0.663 | 0.818 | 0.160 | 0.459 |
| | *F* statistics | 0.950 | 1.605 | 0.159 | 2.454 | 0.773 | 0.919 | 0.204 | 0.419 | 0.203 | 2.012 | 0.810 |
| Day 1 vs. Day 7 | *p* value | 0.482 | 0.448 | 0.635 | 0.484 | 0.309 | 0.282 | 0.542 | 0.692 | 0.553 | 0.045 | 0.316 |
| | *t* statistics | -0.730 | -0.790 | -0.490 | -0.730 | -1.070 | -1.140 | -0.630 | -0.410 | -0.610 | -2.290 | -1.060 |
| | *Hedges' g* | -0.304 | -0.226 | -0.144 | -0.246 | -0.454 | -0.478 | -0.208 | -0.114 | -0.243 | -0.824 | -0.382 |
| Day 7 vs. Day 30 | *p* value | 0.134 | 0.088 | 0.584 | 0.021 | 0.345 | 0.234 | 0.594 | 0.522 | 0.890 | 0.275 | 0.246 |
| | *t* statistics | 1.630 | 1.890 | 0.570 | 2.740 | 0.990 | 1.270 | 0.550 | -0.660 | 0.140 | 1.160 | 1.230 |
| | Hedges' g | 0.433 | 0.491 | 0.176 | 0.698 | 0.365 | 0.341 | 0.138 | -0.163 | 0.041 | 0.456 | 0.348 |
| Day 1 vs. Day 30 | *p* value | 0.588 | 0.371 | 0.957 | 0.216 | 0.930 | 0.920 | 0.903 | 0.473 | 0.692 | 0.526 | 0.935 |
| | *t* statistics | 0.560 | 0.940 | 0.060 | 1.320 | 0.090 | -0.100 | -0.130 | -0.750 | -0.410 | -0.660 | 0.080 |
| | Hedges' g | 0.225 | 0.303 | 0.020 | 0.414 | 0.033 | -0.036 | -0.045 | -0.265 | -0.164 | -0.262 | 0.030 |

*R* = correlation coefficient, STD = standard deviation, L = left, R = right

PCC = posterior cingulate cortex, ACC = anterior cingulate cortex, MeFC = medial frontal cortex, SFG = superior frontal gyrus

IPL = inferior parietal lobule, AG = angular gyrus, Hipp = hippocampus, DMN = default-mode network

2-tail paired *t* tests were performed in all statistical analyses. Degree of freedom = 10.

To account for Bonferroni correction, thresholds of significance: $p \leq 0.0052$ for overall DMN, $p \leq 0.005$ for each node.

l Biomarker in Sports-Related Concussion: Brain Functional Connectivity Alteration of the Default-Mode Network Measured with Longitudinal Resting-State fMRI over 30 Days (doi: 10.1089/neu.2

Table 4. The functional connectivity of the default-mode network of concussed vs. healthy controls: comparing the connectivity to each node from rest of DMN and the overall DMN connectivity

| Days | ROI name | L PCC | L ACC/ MeFC | L SFG | L IPL/AG | L Hipp | R PCC | R ACC/ MeFC | R SFG | R IPL/AG | R Hipp | Overall DMN |
|---|---|---|---|---|---|---|---|---|---|---|---|---|
| Mean of 3 Days for Control | mean of *R* | 0.426 | 0.358 | 0.332 | 0.379 | 0.195 | 0.436 | 0.384 | 0.327 | 0.359 | 0.175 | 0.309 |
| | STD of *R* | 0.066 | 0.090 | 0.083 | 0.078 | 0.059 | 0.065 | 0.081 | 0.082 | 0.065 | 0.059 | 0.057 |
| Day 1[+] vs. Control | *p* value | 0.007 | 0.049 | 0.688 | 0.310 | 0.300 | 0.018 | 0.046 | 0.372 | 0.102 | 0.316 | 0.169 |
| | *t* statistics | 3.04 | 2.12 | -0.41 | 1.05 | 1.07 | 2.63 | 2.15 | -0.92 | 1.73 | 1.03 | 1.44 |
| | Hedges' g | 1.350 | 0.941 | -0.182 | 0.465 | 0.475 | 1.168 | 0.953 | -0.407 | 0.767 | 0.458 | 0.637 |
| Day 7[+] vs. Control | *p* value | 0.041 | 0.093 | 0.004* | 0.007 | 0.001* | 0.016 | 0.065 | 0.001* | 0.0004* | 0.002* | 0.003* |
| | *t* statistics | -2.21 | -1.78 | -3.30 | -3.06 | -4.06 | -2.68 | -1.98 | -4.22 | -4.34 | -3.60 | -3.40 |
| | Hedges' g | -0.982 | -0.791 | -1.466 | -1.360 | -1.801 | -1.190 | -0.877 | -1.871 | -1.925 | -1.600 | -1.511 |
| Day 30[++] vs. Control | *p* value | 0.483 | 0.604 | 0.022 | 0.488 | 0.211 | 0.605 | 0.770 | 0.190 | 0.498 | 0.137 | 0.265 |
| | *t* statistics | -0.72 | -0.53 | -2.54 | -0.71 | -1.30 | -0.53 | -0.30 | -1.37 | -0.69 | -1.57 | -1.15 |
| | Hedges' g | -0.331 | -0.244 | -1.172 | -0.327 | -0.600 | -0.243 | -0.137 | -0.631 | -0.320 | -0.721 | -0.532 |

*R* = correlation coefficient, STD = standard deviation, L = left, R = right

PCC = posterior cingulate cortex, ACC = anterior cingulate cortex, MeFC = medial frontal cortex, SFG = superior frontal gyrus
IPL = inferior parietal lobule, AG = angular gyrus, Hipp = hippocampus, DMN = default-mode network.
[+]Based on all 8 subjects. [++]Based on 7 subjects after removing the one without Day 30 data.
2-tail 2-sample *t* tests were performed in all analyses.
To account for Bonferroni correction, thresholds of significance: $p \leq 0.0052$ for overall DMN, $p \leq 0.005$ for each node.

*Indicates statistically significant.

Table 5. The change of functional connectivity on DMN regions to left isthmus of cingulate cortex based on whole-brain analyses

| | Cluster name | Cluster size ($mm^3$) | Talairach coordinate | Mean *R* on Day 1 | Mean *R* on Day 7 | Cluster name | Cluster size ($mm^3$) | Talairach coordinate | Mean *R* on Day 1 | Mean *R* on Day 7 |
|---|---|---|---|---|---|---|---|---|---|---|
| Day 1 > Day 7[+] | Left PCC/CG/ precuneus | 2611 | (L2,P44,S31) | 0.688 | 0.517 | Right PCC/CG/ precuneus | 2552 | (R3,P52,S17) | 0.651 | 0.463 |
| | Left SFG[*] | 624 | (L7,A35,S52) | 0.258 | -0.033 | Right SFG/MeFC | 1707 | (R2,A31,S53) | 0.239 | -0.068 |
| | Left PHG/ hippocampus | 1402 | (L30,P32,I15) | 0.279 | 0.081 | | | | | |
| | Left AG/MTG/ precuneus | 1193 | (L36,P72,S35) | 0.422 | 0.233 | | | | | |
| | | | | | | | | | | |
| | Cluster name | Cluster size ($mm^3$) | Talairach coordinate | Mean *R* on Day 1 | Mean *R* on Day 30 | | | | | |
| Day 1 > Day 30[++] | Left SFG | 1302 | (L14,A56,S30) | 0.260 | 0.062 | | | | | |
| | | | | | | | | | | |
| Day 30 > Day 7[++] | No significant clusters found in DMN regions. | | | | | | | | | |

PCC = posterior cingulate cortex, CG = cingulate gyrus, SFG = superior frontal gyrus, MeFC = medial frontal cortex, PHG = parahippocampal gyrus

AG = angular gyrus, MTG = middle temporal gyrus

Talairach coordinate indicates the peak statistical location in (R/L, A/P, I/S) format, where R/L = right/left, A/P = anterior/posterior, I/S= inferior/superior.

[+]Based on all 8 subjects. [++] Based on 7 subjects after removing the one without Day 30 data.

[*]This cluster was segmented out from a larger cluster to be anatomically meaningful.

Table 6. The change of functional connectivity on DMN regions to right isthmus of cingulate cortex based on whole-brain analyses

| | Cluster name | Cluster size ($mm^3$) | Talairach Coordinate | Mean *R* on Day 1 | Mean *R* on Day 7 | Cluster name | Cluster size ($mm^3$) | Talairach Coordinate | Mean *R* on Day 1 | Mean *R* on Day |
|---|---|---|---|---|---|---|---|---|---|---|
| Day 1 > Day 7 [+] | Left PCC/CG/ precuneus | 1962 | (L6,P49,S7) | 0.642 | 0.476 | Right PCC/CG/ precuneus | 2325 | (R9,P48,S11) | 0.669 | 0.512 |
| | Left SFG/MeFC/ ACC | 5433 | (L14,A53,S40) | 0.160 | -0.077 | Right SFG [*] | 357 | (R8, A34, S46) | 0.215 | -0.082 |
| | Left PHG/ hippocampus | 2080 | (L23,P16,I11) | 0.250 | 0.035 | | | | | |
| | Left AG/MTG/ precuneus/SOG | 1326 | (L36,P74,S35) | 0.383 | 0.163 | | | | | |
| | | | | | | | | | | |
| Day 1 vs. Day 30 [++] and Day 7 vs. Day 30 [++] | No significant clusters found in DMN regions. | | | | | | | | | |

PCC = posterior cingulate cortex, CG = cingulate gyrus, SFG = superior frontal gyrus, MeFC = medial frontal cortex, ACC = anterior cingulate cortex,

PHG = parahippocampal gyrus, AG = angular gyrus, MTG = middle temporal gyrus, SOG = superior occipital gyrus.

Talairach coordinate indicates the peak statistical location in (R/L, A/P, I/S) format. R/L = right/left, A/P = anterior/posterior, I/S = inferior/superior.

[+]Based on 8 subjects. [++] Based on 7 subjects after removing the one without Day 30 data.

[*]This cluster was segmented out from a larger cluster to be anatomically meaningful.

Table 7. The FA changes from Day 1 to Day 30 after concussion

| | ROI | Corpus callosum | | | Cingulum | | Full skeleton |
|---|---|---|---|---|---|---|---|
| | | Genu | Body | Splenium | Right | Left | |
| Day 1 | mean of FA | 0.743 | 0.678 | 0.763 | 0.571 | 0.587 | 0.401 |
| | STD of FA | 0.023 | 0.011 | 0.022 | 0.020 | 0.025 | 0.012 |
| Day 7 | mean of FA | 0.742 | 0.681 | 0.762 | 0.571 | 0.589 | 0.403 |
| | STD of FA | 0.024 | 0.020 | 0.023 | 0.024 | 0.023 | 0.009 |
| Day 30 | mean of FA | 0.752 | 0.686 | 0.766 | 0.583 | 0.596 | 0.409 |
| | STD of FA | 0.021 | 0.017 | 0.020 | 0.025 | 0.032 | 0.011 |
| ANOVA | *P* value | 0.036 | 0.359 | 0.678 | 0.092 | 0.462 | 0.002 |
| | *F* statistics | 4.420 | 1.119 | 0.401 | 2.935 | 0.825 | 11.772 |
| Day 1 vs. Day 7 | *p* value | 0.877 | 0.668 | 0.869 | 0.974 | 0.683 | 0.497 |
| | *t* statistics | 0.16 | -0.45 | 0.17 | 0.03 | -0.43 | -0.72 |
| | Hedges' g | 0.029 | -0.157 | 0.036 | 0.008 | -0.084 | -0.121 |
| Day 7 vs. Day 30 | *p* value | 0.007 | 0.471 | 0.422 | 0.145 | 0.463 | 0.010* |
| | *t* statistics | -4.02 | -0.77 | -0.86 | -1.68 | -0.78 | -3.68 |
| | Hedges' g | -0.431 | -0.274 | -0.159 | -0.487 | -0.238 | -0.632 |
| Day 1 vs. Day 30 | *p* value | 0.066 | 0.016 | 0.449 | 0.040 | 0.288 | 0.003* |
| | *t* statistics | -2.25 | -3.30 | -0.81 | -2.61 | -1.16 | -4.77 |
| | Hedges' g | -0.413 | -0.539 | -0.127 | -0.512 | -0.304 | -0.674 |

STD = standard deviation, 7 subjects after removing the one without Day 30 data.
2-tail paired *t* tests were performed in all paired wise comparison.
$p \leq 0.05$ is considered significant for full skeleton.
At sub-regions, $p \leq 0.001$ is considered significant to account for Bonferroni correction.
*indicates statistically significant.

l Biomarker in Sports-Related Concussion: Brain Functional Connectivity Alteration of the Default-Mode Network Measured with Longitudinal Resting-State fMRI over 30 Days (doi: 10.1089/neu.2